Applied Physics
Express

The Japan Society
of Applied Physics

LETTER

Hall scattering factors in p-type 4H-SiC with various doping concentrations

To cite this article: Satoshi Asada *et al* 2016 *Appl. Phys. Express* **9** 041301

Applied Physics Express **9**, 041301 (2016)
http://doi.org/10.7567/APEX.9.041301

Hall scattering factors in p-type 4H-SiC with various doping concentrations

Satoshi Asada*, Takafumi Okuda, Tsunenobu Kimoto, and Jun Suda

Department of Electronic Science and Engineering, Kyoto University, Kyoto 615-8510, Japan

*E-mail: asada@semicon.kuee.kyoto-u.ac.jp

Received January 6, 2016; accepted February 16, 2016; published online March 3, 2016

The Hall scattering factor (γ_H) in p-type 4H-SiC with various aluminum doping concentrations of 5.8×10^{14}–$7.1 \times 10^{18}\,\mathrm{cm^{-3}}$ was investigated from 300 to 900 K. γ_H was determined by comparing the Hall coefficient with the theoretical carrier concentration derived from acceptor and donor concentrations obtained from secondary ion mass spectrometry and capacitance–voltage measurements. γ_H decreased with increasing temperature or doping concentration; $\gamma_H = 1$–0.4 for the doping concentration of $5.8 \times 10^{14}\,\mathrm{cm^{-3}}$ and $\gamma_H = 0.5$–0.2 for the doping concentration of $7.1 \times 10^{18}\,\mathrm{cm^{-3}}$. The dependence might be caused by the anisotropic and nonparabolic valence band structure of 4H-SiC.

4H-silicon carbide (4H-SiC) is an attractive semiconductor material for high-power and high-temperature device applications because of its high critical electric field of 2.8 MV/cm and wide bandgap of 3.26 eV.[1,2] Understanding the dependences of electrical properties such as carrier concentration and mobility on temperature and doping concentration in both n- and p-type 4H-SiC is important for designing semiconductor devices or simulating the device characteristics properly. Hall-effect measurement is useful for acquiring such properties, and many studies on n-type 4H-SiC have been reported so far.[3–7] However, only a few studies have been performed for p-type 4H-SiC;[8–11] in particular, knowledge on the Hall scattering factor is very limited.[10,11]

Pensl et al. investigated the temperature-dependent Hall scattering factor of the p-type bulk substrate with an aluminum (Al) doping concentration of $1.2 \times 10^{18}\,\mathrm{cm^{-3}}$ from 100 to 800 K.[10] As a method for obtaining the Hall scattering factor, they compared the Hall-effect measurement results with the theoretical hole concentrations calculated from the net acceptor concentration obtained by secondary ion mass spectrometry (SIMS). The results showed that the Hall scattering factor changes monotonically (1.2–0.6) from 100 to 800 K. The Hall scattering factor in the p-type 4H-SiC bulk substrate was lower than unity at the temperature over 200 K.

In p-type silicon (Si), it had been reported that the hole concentration obtained by Hall-effect measurements (assuming a Hall scattering factor of unity) is higher than the dopant density, suggesting that the Hall scattering factor is below unity.[12,13] Thereafter, it was explained by taking into account the anisotropic and nonparabolic nature of valence band structures. A Hall scattering factor of 0.714–0.882 was theoretically calculated for p-type Si.[14–16] Under a weak magnetic field condition, the Hall scattering factor γ_s is generally obtained by using the relaxation time given by the following equation and becomes between 1 and 2 if the carrier energy in the valence band depends on the wave vector isotropically and parabolically.[14]

$$\gamma_s = \frac{\langle \tau^2 \rangle}{\langle \tau \rangle^2}, \tag{1}$$

where $\langle \tau \rangle$ is the average total relaxation time, and $\langle \tau^2 \rangle$ is the average total square relaxation time. However, the nonparabolic and anisotropic nature of the valence band causes the anisotropy factor γ_a and decreases the Hall scattering factor as follows:[14–16]

$$\gamma_H = \gamma_s \times \gamma_a. \tag{2}$$

Table I. Values obtained by SIMS, Hall-effect, and *C–V* measurements for p-type 4H-SiC samples investigated in this study. For the analyses of Hall-effect measurements, N_A is assumed to be the Al concentration by SIMS measurements.

SIMS	Hall effect (fitted results)				*C–V*
[Al] ($\mathrm{cm^{-3}}$)	N_A ($\mathrm{cm^{-3}}$)	N_D ($\mathrm{cm^{-3}}$)	ΔE_{Al} (eV)	$N_A - N_D$ ($\mathrm{cm^{-3}}$)	$N_A - N_D$ ($\mathrm{cm^{-3}}$)
5.8×10^{14}	(5.8×10^{14})	4.0×10^{13}	0.22	5.4×10^{14}	5.4×10^{14}
1.5×10^{15}	(1.5×10^{15})	1.0×10^{13}	0.21	1.5×10^{15}	1.6×10^{15}
4.6×10^{15}	(4.6×10^{15})	5.0×10^{13}	0.20	4.6×10^{15}	5.3×10^{15}
1.2×10^{16}	(1.2×10^{16})	4.0×10^{13}	0.20	1.2×10^{16}	1.4×10^{16}
2.0×10^{16}	(2.0×10^{16})	1.0×10^{14}	0.20	2.0×10^{16}	2.2×10^{16}
6.5×10^{16}	(6.5×10^{16})	4.0×10^{14}	0.19	6.5×10^{16}	6.7×10^{16}
3.0×10^{17}	(3.0×10^{17})	5.0×10^{14}	0.19	3.0×10^{17}	3.1×10^{17}
5.5×10^{17}	(5.5×10^{17})	2.0×10^{15}	0.18	5.5×10^{17}	6.0×10^{17}
7.1×10^{18}	(7.1×10^{18})	1.2×10^{16}	0.17	7.1×10^{18}	7.0×10^{18}

Pensl et al. provided important data for the Hall-effect measurement in the p-type 4H-SiC.[10] For example, Parisini and Nipoti analyzed heavily doped p-type 4H-SiC layers formed by $\mathrm{Al^+}$ ion implantation by using Pensl et al.'s Hall scattering factor.[11] However, there is only one experimental data for the p-type 4H-SiC and it is worth obtaining a better understanding of the Hall scattering factor by utilizing samples with various doping concentrations. In this study, we conducted the Hall-effect measurement on the p-type 4H-SiC homoepitaxial layers from 160 to 900 K with a wide range of Al doping concentrations of 5.8×10^{14}–$7.1 \times 10^{18}\,\mathrm{cm^{-3}}$. The dependence of the Hall scattering factor on the temperature as well as the Al doping concentration was investigated by using the same method as that in Pensl et al.'s work.[10] In addition to homoepitaxial layers, the experiment and analysis were performed on a p-type 4H-SiC bulk substrate with an Al concentration of $1.0 \times 10^{18}\,\mathrm{cm^{-3}}$.

The structure of the measured samples was as follows: 100-μm-thick Al-doped p-type 4H-SiC epilayers were grown on n-type 4H-SiC(0001) 4°-off-axis substrates by chemical vapor deposition. Nine samples with different Al concentrations were prepared. The Al concentrations measured by SIMS are summarized in Table I. We confirmed that the densities of boron (B), which acts as a deep acceptor in 4H-SiC,[17] were below the detection limit of SIMS ($10^{13}\,\mathrm{cm^{-3}}$) in all nine samples. Nitrogen (N), which acts as a compensating shallow donor,[17] was also measured in the two samples whose Al concentrations were 1.5×10^{15} and 2.0×10^{16} cm^{-3}. The N concentrations in both samples were confirmed to be below the detection limit (5.0×10^{15} cm^{-3}). The samples were cut into 5×5 mm^2. Highly doped p-type regions were formed to obtain good ohmic contacts only beneath the four corners. These regions were formed by high-temperature Al$^+$ implantation (3.0×10^{20} cm^{-3}, 200 nm box profile) at 500 °C with subsequent activation annealing at 1700 °C for 15 min. Ti/Al (50/200 nm) electrodes were deposited on the four corners, and contact annealing at 1000 °C for 2 min was performed.

Hall-effect measurement by the van der Pauw method was performed on the samples from 160 to 900 K under a magnetic field of 0.515 T by using a Hall-effect measurement system (Nanometrics HL5550 for 160–300 K, HL5590 for 300–900 K). The applied voltage for current flow was set to be below 6 V and the measurement current was increased from 0.8 μA to 20 mA with increasing temperature. Since the p-epilayers of the samples were grown on the n-type substrate, the effect of leakage current of the vertical p–n junction should be considered. We confirmed that the reverse leakage current of the p–n junction was small enough to neglect as follows. The vertical p–n junction leakage current at −6 V increased with temperature from <1 nA (detection limit) at RT to 0.1 mA at 900 K, which was below one-thousandth of the measurement current at a temperature lower than 800 K and below one-hundredth at 900 K. To obtain the net acceptor concentrations of the samples, C–V measurements on Ti/p-SiC Schottky structures were also performed.

The method used for the determination of the Hall scattering factor was the same as that in Pensl et al.'s study.[10] In the Hall-effect measurement, the hole concentration p can be derived from the Hall coefficient as

$$p = \frac{\gamma_H}{qR_H}, \qquad (3)$$

where γ_H is the Hall scattering factor for holes, q is the elementary charge, and R_H is the Hall coefficient. Therefore, the Hall scattering factor can be determined by comparing the hole concentration obtained by Hall-effect measurement assuming the Hall scattering factor of unity ($p_{\rm Hall}$) with the theoretical hole concentration ($p_{\rm theory}$) calculated from the semiconductor statistics.

Figure 1 shows the Arrhenius plot of the hole concentrations from 160 to 900 K. Symbols denote the hole concentrations obtained by Hall-effect measurement assuming the Hall scattering factor as unity ($p_{\rm Hall}$). The solid lines depicted in Fig. 1 express the theoretical hole concentrations ($p_{\rm theory}$) of the representative samples whose doping concentrations were 5.8×10^{14}, 2.0×10^{16}, 3.0×10^{17}, and 7.1×10^{18} cm^{-3}. The theoretical values were calculated assuming a single ionized acceptor and a compensating donor as

$$p + N_D = \frac{N_A}{1 + \dfrac{g(T)p}{N_V(T)} \exp\left(\dfrac{\Delta E_{\rm Al}}{k_B T}\right)}, \qquad (4)$$

where T is the absolute temperature, N_A is the acceptor concentration, N_D is the compensating donor concentration, $\Delta E_{\rm Al}$ is the ionization energy of the Al acceptor, $g(T)$ is the temperature-dependent acceptor degeneracy factor, N_V is the effective density of states in the valence band, and k_B is the Boltzmann constant. These parameters were assigned as follows:

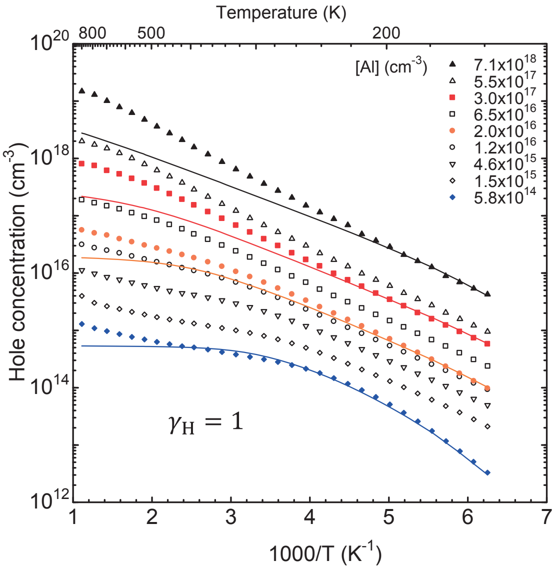

Fig. 1. Temperature dependence of the hole concentration from 160 to 900 K in p-type 4H-SiC. The symbols indicate measurement values while assuming the Hall scattering factor of unity and the solid lines denote theoretical values calculated from semiconductor statistics.

The Al concentrations in the epilayers measured by SIMS were applied to the acceptor concentration N_A. The compensating donor concentration N_D and the ionization energy $\Delta E_{\rm Al}$ were considered fitting parameters since the N concentration could not be measured by SIMS owing to the detection limit. The fitting was performed below 250 K, in the freeze-out region, where the theoretical values are very sensible to the fitting parameters N_D and $\Delta E_{\rm Al}$. The results of the fitting are shown in Table I. N_D was consistent with the SIMS measurement results (N was below the detection limit of 5.0×10^{15} cm^{-3}) except for the sample with an acceptor concentration of 7.1×10^{18} cm^{-3}. This misfit was attributed to the high hole concentration even at a temperature of 160 K. $\Delta E_{\rm Al}$ decreased from 0.22 to 0.17 eV with increasing doping concentration, which agreed with previous reports.[9,18,19] The previous reports showed the same dependence of the ionization energy on the Al doping concentration and became 0.24–0.16 eV with increasing Al doping concentration from 10^{15} to 10^{19} cm^{-3}.

For the fitting described above, the excited states of the Al acceptor, based on a hydrogenic model, were included to derive the temperature-dependent acceptor degeneracy factor $g(T)$.[8,9] The increase in the number of the energy states for the hole in the forbidden band causes the increase in degeneracy factor as in the following equation, resulting in a low ionization ratio:

$$g_n(T) = g_A \times \left[1 + \sum_{r=2}^{n} g_r \exp\left(\frac{\Delta E_r - \Delta E_{\rm Al}}{k_B T}\right)\right], \qquad (5)$$

where g_A is the acceptor degeneracy factor of 4, ΔE_r is the energy separation between the valence band and the $(r-1)$th excited states, n is the highest excited state number, and g_r is the $(r-1)$th excited state degeneracy factor, which is expressed as r^2. ΔE_r is described as

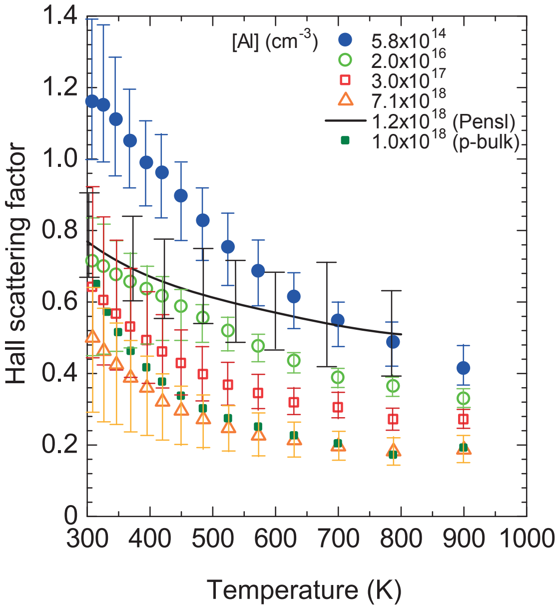

Fig. 2. Temperature dependence of Hall scattering factor for holes from 300 to 900 K in p-type 4H-SiC. The solid black line expresses Pensl et al.'s data and the green square points show the Hall scattering factor in a bulk substrate.

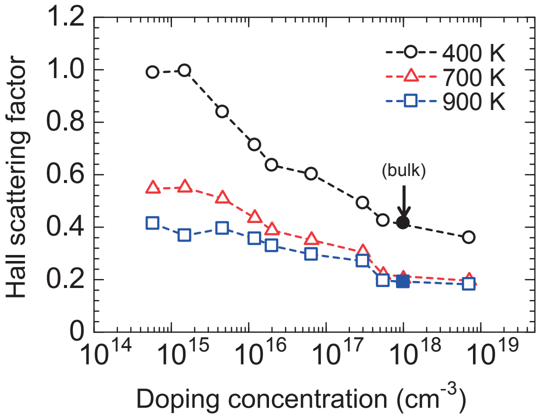

Fig. 3. Dependence of Hall scattering factor for holes on the doping concentration of Al acceptor in p-type 4H-SiC.

$$\Delta E_r = \frac{q^4 m_h^*}{8h^2\epsilon_0^2\epsilon_s^2 r^2}, \tag{6}$$

where m_h^* is the hole effective mass, which is assumed to be the same as the rest electron mass for simplicity, h is the Planck constant, ϵ_0 is the vacuum permittivity, and ϵ_s is the static dielectric constant, which was assumed to be 9.7. In this study, we set the highest excited state number n in Eq. (5) to be maximum so that the Bohr radius of the excited state does not exceed half of the average distance of the neighboring Al atom. For example, $n = 11$ and 2 were used for the acceptor concentrations of 5.8×10^{14} and 7.1×10^{18} cm^{-3}, respectively. The effective density of states, $N_V(T)$, was determined to be $2.1 \times 10^{19} \times (T/300)^{3/2}$ cm^{-3}.[20)]

To confirm the correctness of N_A and N_D obtained by Hall-effect measurement, capacitance–voltage (C–V) measurement on Ti/p-SiC Schottky structures was performed in all the samples. As shown in Table I, the net acceptor concentrations $N_A - N_D$ obtained by C–V measurement were in excellent agreement with the Hall-effect measurement results, suggesting high accuracy in the determination of N_A in all the samples.

The Hall scattering factor can be derived from $\gamma_H = p_{\text{theory}}/p_{\text{Hall}}$, as shown in Fig. 2. Here, we focused on the Hall scattering factors above 300 K, near or in the saturation regime, because the values at temperatures below 300 K were less accurate owing to the strong dependence on the ambiguous fitting parameters. Even at temperatures above 300 K, error bars, which were attributed to the fitting parameters of N_D and ΔE_{Al}, existed. The fitting parameters for the determination of the error bars ranged from $N_D = 0$ to 1.0×10^{14} cm^{-3} and from $\Delta E_{\text{Al}} = 0.19$ to 0.23 eV for the doping concentration of 5.8×10^{14} cm^{-3}. For the doping concentration of 7.1×10^{18} cm^{-3}, they ranged from $N_D = 0$ to 1.2×10^{16} cm^{-3} and from $\Delta E_{\text{Al}} = 0.16$ to 0.20 eV. The error of the present estimation became significantly smaller with increasing temperature because the theoretical hole concentration is determined almost uniquely by the net acceptor concentration at high temperatures. As mentioned above, we performed both SIMS and C–V measurements to cross check the net acceptor concentrations in all the samples.

The Hall scattering factors were eventually smaller than unity and decreased further with increasing temperature, which was the same tendency as in Pensl et al.'s report, as depicted by a black solid line with error bars in Fig. 2.[10)] However, our Hall scattering factors in the epilayers whose doping concentrations were 5.5×10^{17} and 7.1×10^{18} cm^{-3}, similar to the concentrations in Pensl et al.'s work, were not in the error bar of Pensl et al.'s data. Since we confirmed the correctness of the Hall scattering factor carefully by SIMS and C–V measurements, the present results may give more reliable values. To support this, however, accurate theoretical studies are required.

The decrease in Hall scattering factor with increasing temperature might be caused by a stronger effect of the anisotropy factor γ_a in Eq. (2) at high temperatures. At high temperatures, the ratio of high-energy hole density increases, which emphasizes the effect of the anisotropy factor due to the strong nonparabolicity and anisotropy at the high-energy state in the valence band.[21)]

The previous studies[10,11)] assumed that the Hall scattering factor depends on the temperature but does not depend on the doping concentration. As seen in Fig. 3, however, our results clearly demonstrated the decrease in Hall scattering factor with increasing doping concentration and took a very low value of 0.2 at 900 K for the doping concentration of 7.1×10^{18} cm^{-3}. Although the reason for this behavior has not been revealed yet, this is the first observation of a clear dependence of the Hall scattering factor on the Al doping concentration in SiC.

To examine the effect of the growth method on the Hall scattering factor, the temperature dependence of the Hall scattering factor in a p-type 4H-SiC bulk substrate (grown by sublimation) was also investigated. By SIMS measurement, the Al acceptor concentration was 1.0×10^{18} cm^{-3}, the B concentration was 1.0×10^{17} cm^{-3} (only 10% of the Al concentration), and the N concentration was below the detection limit in the bulk substrate. As shown in Figs. 2 and 3, the Hall scattering factor in the bulk substrate was almost identical to that in the epilayers. Although the growth method and the density of unwanted impurities and deep levels of the bulk substrate are different from those of the epilayers, almost the same result was obtained. This indicates that the dependences of the Hall scattering factor on the temperature and doping concentration obtained in this study are common in p-type 4H-SiC.

In conclusion, the temperature dependences of the Hall scattering factor in p-type 4H-SiC epilayers with various Al doping concentrations from 5.8×10^{14} to $7.1 \times 10^{18}\,\mathrm{cm}^{-3}$ and in the bulk substrate whose doping concentration was $1.0 \times 10^{18}\,\mathrm{cm}^{-3}$ were investigated. Careful investigation based on the SIMS and C–V measurements revealed that the Hall scattering factor decreased to 0.2 with increasing doping concentration and temperature to $7.1 \times 10^{18}\,\mathrm{cm}^{-3}$ and 900 K, respectively. This work provided important knowledge for the analyses of the electrical properties of p-type 4H-SiC by Hall-effect measurement.

1) M. Bhatnagar and B. J. Baliga, IEEE Trans. Electron Devices **40**, 645 (1993).
2) A. Itoh, T. Kimoto, and H. Matsunami, IEEE Electron Device Lett. **16**, 280 (1995).
3) W. Götz, A. Schöner, G. Pensl, W. Suttrop, W. J. Choyke, R. Stein, and S. Leibenzeder, J. Appl. Phys. **73**, 3332 (1993).
4) J. Pernot, S. Contreras, J. Camassel, J. L. Robert, W. Zawadzki, E. Neyret, L. Di Cioccio, U. Umr, and M. Cedex, Appl. Phys. Lett. **77**, 4359 (2000).
5) H. Iwata and K. M. Itoh, J. Appl. Phys. **89**, 6228 (2001).
6) J. Pernot, W. Zawadzki, S. Contreras, J. L. Robert, E. Neyret, and L. Di Cioccio, J. Appl. Phys. **90**, 1869 (2001).
7) G. Rutsch, R. P. Devaty, D. W. Langer, L. B. Rowland, and W. J. Choyke, J. Appl. Phys. **84**, 2062 (1998).
8) H. Matsuura, J. Appl. Phys. **95**, 4213 (2004).
9) A. Koizumi, J. Suda, and T. Kimoto, J. Appl. Phys. **106**, 013716 (2009).
10) G. Pensl, F. Schmid, F. Ciobanu, M. Laube, S. A. Reshanov, N. Schulze, K. Semmeiroth, H. Nagasawa, A. Schöner, and G. Wagner, Mater. Sci. Forum **433–436**, 365 (2003).
11) A. Parisini and R. Nipoti, J. Appl. Phys. **114**, 243703 (2013).
12) P. P. Debye and T. Kohane, Phys. Rev. **94**, 724 (1954).
13) D. K. Schroder, T. T. Braggins, and H. M. Hobgood, J. Appl. Phys. **49**, 5256 (1978).
14) J. F. Lin, S. S. Li, L. C. Linares, and K. W. Teng, Solid-State Electron. **24**, 827 (1981).
15) B. Lax and J. G. Mavroides, Phys. Rev. **100**, 1650 (1955).
16) R. S. Allgaier, Phys. Rev. **158**, 699 (1967).
17) M. Ikeda, H. Matsunami, and T. Tanaka, Phys. Rev. B **22**, 2842 (1980).
18) H. Matsuura, M. Komeda, S. Kagamihara, H. Iwata, R. Ishihara, T. Hatakeyama, T. Watanabe, K. Kojima, T. Shinohe, and K. Arai, J. Appl. Phys. **96**, 2708 (2004).
19) J. Pernot, S. Contreras, and J. Camassel, J. Appl. Phys. **98**, 023706 (2005).
20) T. Kimoto and J. A. Cooper, *Fundamentals of Silicon Carbide Technology* (Wiley, Singapore, 2014).
21) C. Persson and U. Lindefelt, J. Appl. Phys. **82**, 5496 (1997).